Producing Large-Sized, Skew Bevel Gear Pinion Using Multi-Axis Control and Multi-Tasking Machine Tool

I. Tsuji, K. Kawasaki and H. Gunbara

This paper proposes a method for the manufacture of a replacement pinion for an existing, large-sized skew bevel gear using multi-axis control and multitasking machine tool.

Introduction

Bevel gears are used to transmit power and motion between the intersecting axes of two shafts, most often mounted on shafts 90° apart. They may have straight, Zerol, spiral or skew teeth (Refs. 1–4), and are common in gear transmissions (Ref. 5).

The transmission of straight bevel gears is regarded as a particular case of skew bevel gears (Ref. 6) in that their contact ratio is larger than that of straight bevel gears and skew bevel gears have oblique teeth.

Skew bevel gears are typically used in power generation plants and are quite large. In recent years these mostly aging plants have been undergoing extensive retrofitting and so it has often become necessary to replace the skew bevel gears used in them. In some cases, where only the pinion member is changed, it then becomes necessary to manufacture a new pinion that performs well with the existing gear member.

It is now possible to machine these gears' complicated tooth surface due to the development of multi-axis control and multitasking machine tools (Refs. 7–8). Therefore, high-precision machining of large-sized, skew bevel gears has become commonplace.

Proposed here is a method for manufacturing new pinion mates for large-sized, skew bevel gears using multi-axis control and multitasking machine tools. This manufacturing method has the dual advantages of arbitrary modification of the tooth surface and of machining the part without the tooth surface (Ref. 9).

To begin, understand that the tooth surface forms of skew bevel gears are modeled mathematically. Next, the real tooth surfaces of the gear member are measured using a coordinate measuring machine (CMM), and the deviations between the real and theoretical tooth surface forms are formalized using the measured coordinates. It is now possible to analyze the tooth contact pattern and transmission errors of the skew bevel gears while addressing the deviations of the real and theoretical tooth surface forms by expressing the deviations as polynomial equations.

The components of the deviations of tooth surface forms corresponding to the distortions of heat treatment and lapping, etc., are used because the motion concept can be implemented on the multitasking machine.

Further, deviations of the tooth surface forms of the gear member can be reflected in the analysis of the tooth contact pattern and transmission errors, and the tooth surface form of the pinion member that has good performance mating with the existing gear member is determined. Finally, the pinion member is manufactured by a swarf cutting that is machined using the side of the end mill of a multi-axis control and multitasking machine tool. Afterward, the real tooth surfaces of the manufactured pinion member are measured using a CMM and the tooth surface form errors are detected. Although the tooth surface form errors were especially large on the coast-side, they are in fact minimal on the drive-side. In addition, the tooth contact pattern of the manufactured pinion member and the provided original gear member were compared with the results from tooth contact analysis (TCA), and there was good agreement.

Tooth Surfaces of Skew Bevel Gears

As mentioned, the tooth surface forms of skew bevel gears are modeled mathematically. In general, the geometry of the skew bevel gears is achieved by considering the complementary crown gear as the theoretical generating tool. Therefore, the tooth surface form of the complementary crown gear is considered first.

The number of teeth of the complementary crown gear is represented by:

$$z_c = \frac{z_p}{\sin \lambda_{p0}} = \frac{z_g}{\sin \lambda_{g0}} \tag{1}$$

where:

z_c is number of teeth of complementary crown gear
z_p is number of teeth of the pinion
z_g is number of teeth of the gear
λ_{p0} is pitch cone angles of the pinion
λ_{g0} is pitch cone angles of the gear

Figure 1 shows the tooth surface form of the complementary crown gear assuming to be straight bevel gears with depth-wise tooth taper. O-xyz is the coordinate system fixed to the crown gear and the *z* axis is the crown gear axis of rotation. Point P is a reference point at which tooth surfaces mesh with each other and is defined in the center of the tooth surface. The circular arcs with large radii of curvatures are defined both in xz and xy planes; the xz and xy planes correspond to the sections of the tooth profile and tooth trace of the tooth surface, respectively.

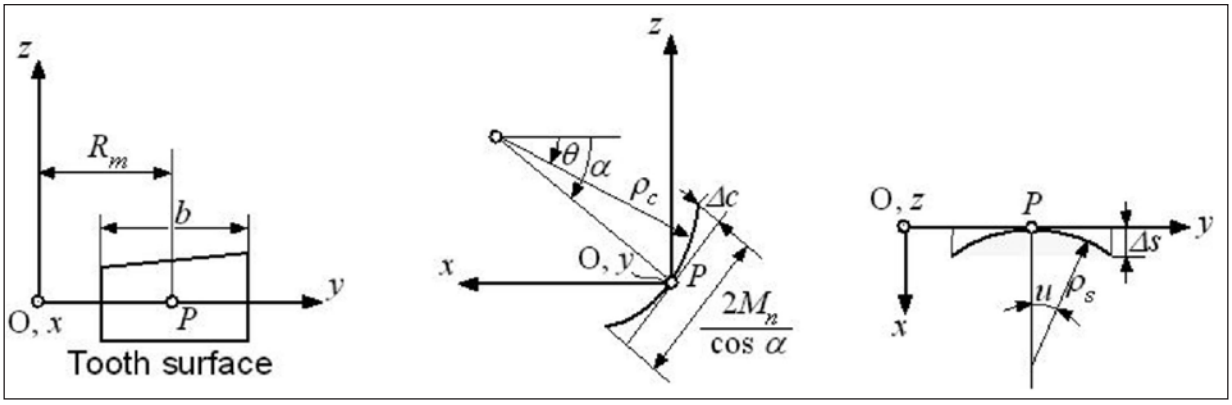

Figure 1 Tooth surface form of complementary crown gear.

This curved surface is defined as the tooth surface of the complementary crown gear. The following equations demonstrate the relations between ρ_c, Δc and M_n in xz, and between ρ_s, Δs and b in xy planes, respectively (Ref. 10).

Since skew bevel gears have teeth that are straight and oblique, the skew bevel gear has in fact a skew angle (Fig. 2). Thus the complementary crown gear also has the skew angle, defined as β. The tooth surface of the complementary crown gear is expressed in O-xyz using ρ_c and ρ_s:

$$\rho_c = \frac{\Delta c^2 + \left(\frac{M_n}{\cos\alpha}\right)^2}{2\Delta c} \tag{2}$$

$$\rho_s = \frac{\Delta s^2 + \frac{b^2}{4}}{2\Delta s}$$

where:

ρ_c = radius of the curvature of the circular arcs in the xy plane, and has influence on Δc
Δc = amount of tooth profile modification
M_n = normal module
α = pressure angle
ρ_s = radius of curvature of the circular arcs in the xy plane, and influence on Δs
Δs = amount of tooth profile crowning
b = facewidth

$$X(u,\theta) = \begin{bmatrix} -\rho_c(\cos\theta - \cos\alpha) - \rho s(1 - \cos u) + \rho_s \sin u \tan\beta \\ \rho_s \sin u + R_m \\ \rho_c(\sin\alpha - \sin\theta) \end{bmatrix} \tag{3}$$

where:

X = position vector of tooth surface of complementary crown gear in O-xyz
u = parameter which represents curved lines
θ = parameter which represents curved lines
R_m = mean cone distance

The unit-normal X is expressed by N.

The equation of the tooth surface of the complementary crown gear = X. The complementary crown gear is rotated about the z axis by angle ψ and generates the tooth surface of the skew- bevel gear. This rotation angle — ψ — of the crown gear, is the generating angle. When the generating angle is ψ, X and N are rewritten as $X\psi$ and $N\psi$ in O-$x_s y_s z_s$, assuming that the coordinate system O-xyz is rotated about the z axis by ψ in the coordinate system O-$x_s y_s z_s$ and is fixed in space. When ψ is zero, O-$x_s y_s z_s$ coincides with O-xyz.

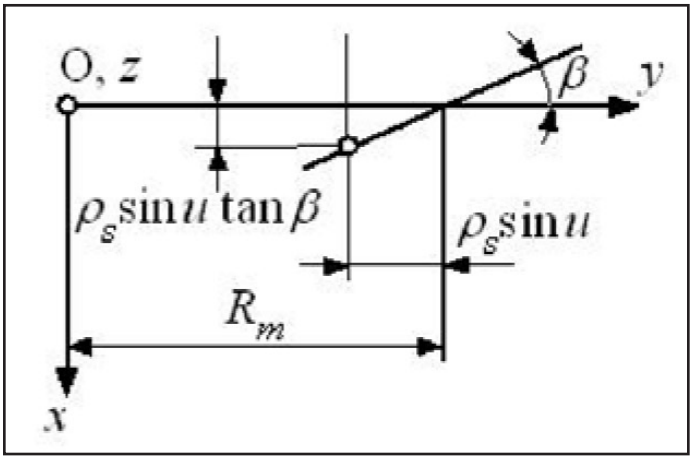

Figure 2 Skew angle of complementary crown gear.

Assuming the relative velocity W ($X\psi$) between the crown gear and the generated gear at the moment when generating angle is ψ, the equation of meshing between the two gears is as follows (Refs. 11–12):

$$N_\psi(u, \theta; \psi)\, W(u, \theta; \psi) = 0 \tag{4}$$

where:

$N\psi$ = the unit-normal vector of $X\psi$ in O-$x_s y_s z_s$
$X\psi$ = position vector of tooth surface of complementary crown gear in O-$x_s y_s z_s$
ψ = parameter representing rotation angle of complementary crown gear about the z axis

From Equation 4 we have θ = θ (u,ψ). Substituting θ (u,ψ) into $X\psi$ and $N\psi$, any point on the tooth surface of the crown gear and its unit-normal are defined by a combination of (u,ψ), respectively. When the tooth surface of the complementary crown gear in O-$x_s y_s z_s$ is transformed into the coordinate system fixed to the generated gear, the tooth surface of the skew-bevel gear is expressed. The tooth surfaces of the pinion and gear are expressed as x_p and x_g, respectively. Moreover, the unit-normals of x_p and x_g are expressed as n_p and n_g, respectively. Henceforth, the subscripts "p" and "g" indicate that each is related to the pinion and gear.

Measurement of Gear Member

Manufacturing errors occur in bevel gear cutting, sometimes because whether the mathematical model, as mentioned earlier,

fits the real tooth surface of the existing gear member or not, is not obvious. Therefore the tooth surfaces of the gear member are measured using a CMM and the deviations between the real and theoretical tooth surface forms are formalized.

Coordinate measurement of real tooth surface. The theoretical tooth surfaces of the gear member are expressed as x_g (u_g,ψ_g), as mentioned. A grid of n lines and m columns is defined and a point — or reference point — is specified on the tooth surfaces of both the drive- and coast-sides; the reference point is usually plotted in the center of the grid. The position vectors x_g (x, y, z) — namely, u, θ and ψ — are determined for the solution of simultaneous equations by considering one point on the grid of the tooth surface; the unit-normal (n_x, n_y, n_z) of the corresponding surface point is also determined since u, θ and ψ are determined (Ref. 13).

For measurement, the gear member is set up arbitrarily on a CMM whose coordinate system is defined as Om-$x_m y_m z_m$. We can make origin O_m and axis z_m coincide with the origin and the axis of the gear member, respectively. The whole grid of surface points, together with the theoretical tooth surfaces, is rotated about the z_m axis so that y_m is equal to zero at the reference point. Therefore, the position vector of the point and its unit-normal are transformed into the coordinate system O_m-$x_m y_m z_m$ and are represented by:

$$x^{(i)} = \left(x^{(i)}, y^{(i)}, z^{(i)}\right)^T \quad (i = 1, 2, \ldots, 2nm)$$
$$n^{(i)} = \left(n_x^{(i)}, n_y^{(i)}, n_z^{(i)}\right)^T \quad (5)$$

where:

$x^{(i)}$ is the position vector of the *i-th* point of tooth surface in O_m- $x_m y_m z_m$

$n^{(i)}$ is the unit-normal vector of $x^{(i)}$

The real tooth surface of the gear member was measured using a CMM (Sigma M and M3000 developed by Gleason Works). When the real tooth surface is measured according to the provided grid, the *i-th*-measured tooth surface coordinates are obtained and numerically expressed as the position vector (Refs. 13–14):

$$x_m^{(i)} = \left(x_m^{(i)}, y_m^{(i)}, z_m^{(i)}\right)^T \quad (i = 1, 2, \ldots, 2nm) \quad (6)$$

where:

$X_m^{(i)}$ is the position vector of the *i-th*-measured tooth surface coordinates in O_m-$x_m y_m z_m$

When the deviation δ between the measured coordinates and nominal data of the theoretical tooth surfaces for each point on the grid is defined towards the direction of the normal of the theoretical tooth surface, *i-th* δ can be determined by:

$$\delta^{(i)} = \left(x_m^{(i)} - x^{(i)}\right) n^{(i)} \quad (i = 1, 2, \ldots, 2nm) \quad (7)$$

where:

the deviation between measured coordinates and nominal data of tooth surface is $\delta^{(i)}$ for each point on the grid towards the direction of the normal of tooth surface; δ is equal to zero at the reference point.

The fundamental components of the deviations of tooth surface forms corresponding with the distortions of heat treatment and lapping, etc., are used because the motion concept may be implemented on a multitasking machine.

Formalization of deviations of tooth surface form. Based on the method mentioned earlier, the deviation δ for each point on the grid is calculated when the points on the tooth surface are measured (Ref. 15). However, it is difficult to ideally fit δ to the theoretical tooth surface because δ varies at each point on the grid. We therefore define (X, Y) whose X and Y are toward the directions of the tooth profile and tooth trace, respectively, and form the following polynomial expression:

$$\delta = \delta_{11} + \delta_{12} + \delta_{21} + \delta_{22} + \delta_{31} + \delta_{32} + \delta_{41} \quad (8)$$

where:

δ_{11} = parameter-defining deviation
δ_{12} = parameter-defining deviation
δ_{21} = parameter-defining deviation
δ_{22} = parameter-defining deviation
δ_{31} = parameter-defining deviation
δ_{32} = parameter-defining deviation
δ_{41} = parameter-defining deviation

Figure 3 shows the procedure formalizing the relation between the fundamental components of polynomial expression and the deviation of tooth surface form. First, the tooth trace deviation δ_{11} and tooth profile deviation δ_{12} are expressed as the following first-order equations of X and Y, using fundamental components a_{11} and a_{12}, respectively (Fig. 3a):

$$\delta_{11} = a_{11} X$$
$$a_{11} = \frac{\delta_{11}}{0.5\,H} \quad (9)$$
$$\delta_{12} = a_{12} Y$$
$$a_{12} = \frac{\delta_{11}}{0.5\,T}$$

where:

a_{11} = fundamental component of polynomial expression
H = range of the evaluation of the tooth surface in X directions
a_{12} = fundamental component of polynomial expression
T = range of the evaluation of the tooth surface in Y directions

The tooth trace deviation δ_{21} and tooth profile deviation δ_{22} are expressed as the following second-order equations of both X and Y, using fundamental components a_{21} and a_{22}, respectively (Fig. 3b):

$$\delta_{21} = a_{21} X^2$$
$$a_{21} = \frac{\delta_{21}}{(0.5\,H)^2} = \frac{4\,\delta_{21}}{H^2} \quad (10)$$
$$\delta_{22} = a_{21} Y^2$$
$$a_{22} = \frac{\delta_{22}}{(0.5\,T)^2} = \frac{4\,\delta_{22}}{T^2}$$

where:

a_{21} = fundamental component of polynomial expression
a_{22} = fundamental component of polynomial expression

Further, the deviations δ_{31} and δ_{32} in the directions of the bias-in and bias-out are expressed as the following second-order equations of both X and Y, using fundamental components a_{31} and a_{32}, respectively (Fig. 3c):

$$\xi_1 = \tan^{-1}\left(\frac{T}{H}\right), \; L_0 = \frac{H}{\cos \xi_1} \quad (11)$$

$$\delta_{31} = a_{31} (X \cos \xi_1 - Y \sin \xi_1)^2$$

$$a_{31} = \frac{\delta_{31}}{(0.5\, L_0)^2} = \frac{4\, \delta_{31}}{H_0^2}$$

$$\delta_{32} = a_{32} (X \cos \xi_1 - Y \sin \xi_1)^2$$

$$a_{32} = \frac{\delta_{32}}{(0.5\, L_0)^2} = \frac{4\, \delta_{31}}{L_0^2}$$

where:

a_{31} = fundamental component of polynomial expression

a_{32} = fundamental component of polynomial expression

The tooth trace deviation δ_{41} is expressed as the following third-order equations of X and Y, using fundamental components b_1, b_2 and b_3, respectively (Fig. 3d):

$$\delta_{41} = b_3 X^3 + b_2 X^2 + b_1 X \quad (12)$$

Thus b_1, b_2 and b_3 are determined from the following conditions: δ is equal to zero when $X = -0.5H$ and $X = 0.5H$. In addition, δ is equal to δ_{41} when $X = 0.25H$. Reflecting the polynomial expression δ to the theoretical tooth surface, the position vector is represented by:

$$x_a = x + \delta\, n \quad (13)$$

Thus x_a describes the theoretical tooth surface with consideration of the tooth surface form deviations. The tooth contact patterns and transmission errors with the tooth surface form deviations are analyzed using x_a. The position vector of the *i-th* point of the theoretical tooth surface is expressed as $x_a^{(i)}$.

Formalization of Measured Results

The real tooth surfaces of the gear member to be used were measured on a CMM and the deviations between the real and theoretical tooth surface forms were formalized. Table 1 shows the dimensions of the skew bevel gears. The pitch circle diameter of the gear member is 1,702.13 mm — very large. Five points in the direction of the tooth profile and nine points in the direction of the tooth trace for the grid were used. Figure 4 shows the formalized results of the measured coordinates. Figure 4a shows the measured results using a CMM compared to the theoretical tooth surface. Figure 4b shows the formalized results using Equations 9, 10 and 11 in Equation 8. Figure 4c shows the formalized results using Equation 12, in addition to Equations 9, 10 and 11 in Equation 8. The maximum values of the magnitude of deviations are 0.793 mm, 0.128 mm and 0.066 mm in Figure 4a, b and c, respectively. The overall deviations gradually decrease as a whole from Figure 4a and 4c. As the deviations are formalized with a large number of equations, the deviations decrease and fit the measured coordinates well to the theoretical tooth surface. Therefore, once formalization of the deviations was validated the fundamental components of the deviations of the tooth surface forms corresponded to the distortions of heat treatment and lapping, etc.

Tooth Contact Analysis (TCA)

Concept of tooth contact analysis. The tooth surface form of the pinion member that has good performance mating with the existing gear member mentioned earlier is considered based on tooth contact analysis. In this case, the tooth surface form of the

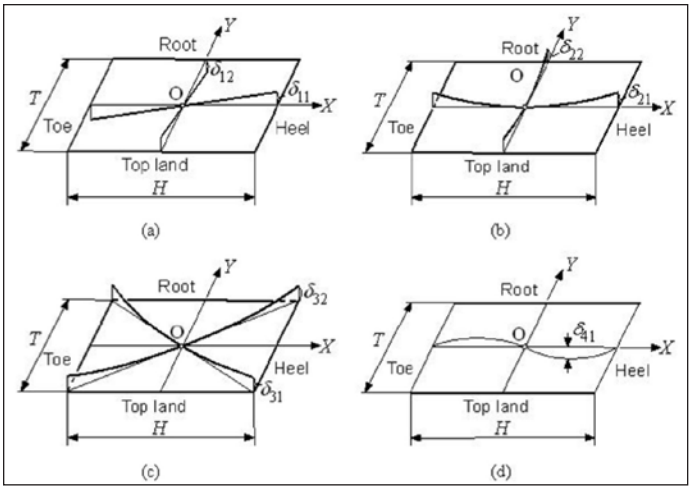

Figure 3 Procedure formalizing relation between fundamental components of polynomial expression and deviation of tooth surface form.

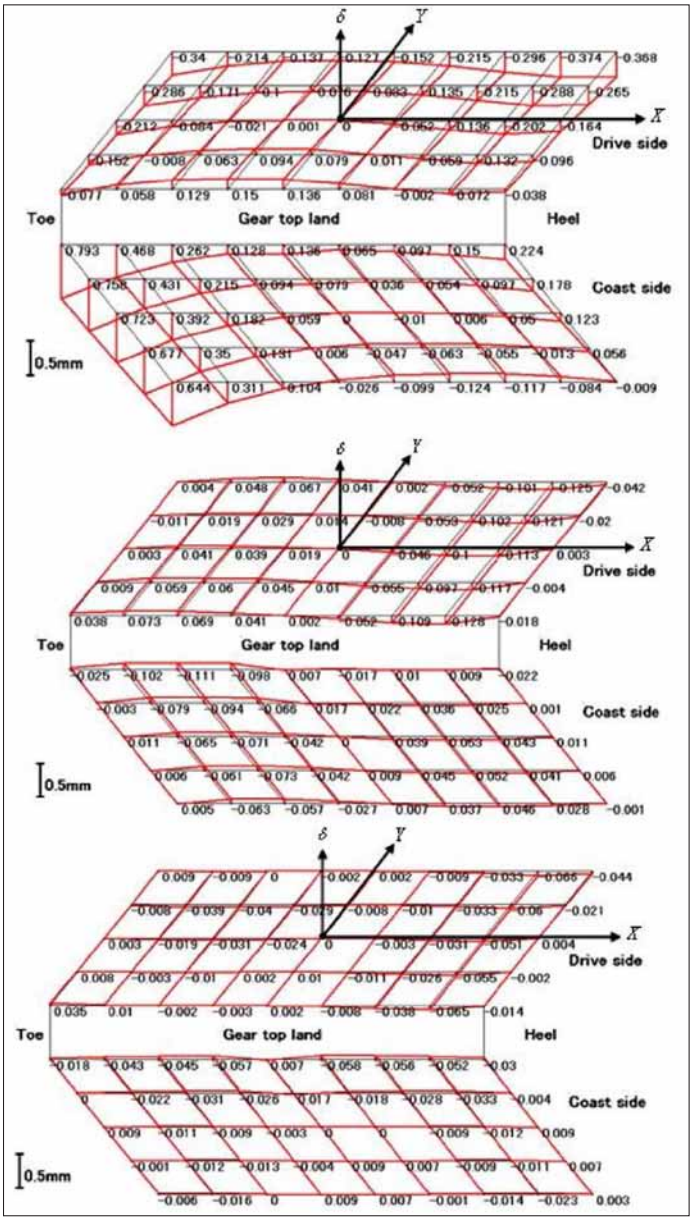

Figure 4 Formalized results based on measured coordinates.

pinion member is modeled using Equation 1and the appropriate amount of profile modification and crowning is calculated.

The pinion and gear members are assembled in a coordinate system O_h-$x_h y_h z_h$ (Fig. 5) in order to analyze the tooth contact pattern and transmission errors of the pinion member and existing gear member. Suppose that φ_p and φ_g are the rotation angles of the pinion and gear, respectively. The position vectors of the pinion and gear tooth surfaces must coincide and the direction of two unit-normals at this position must be also agree in order to contact the two surfaces. Therefore, the following equations yield:

$$B(\varphi_p)\, x_p(u_p, \psi_p) = C(\varphi_g)\, x_g(u_g, \psi_g)$$
$$B(\varphi_p)\, n_p(u_p, \psi_p) = C(\varphi_g)\, n_g(u_g, \psi_g) \quad (14)$$

where:

B and *C* are the coordinate transformation matrices for the rotation about the y_h and z_h axes, respectively

φ_p is the rotation angle of pinion about *yh* axis in O_h-$x_h y_h z_h$

φ_g is the rotation angle of gear about *zh* axis in O_h-$x_h y_h z_h$ (15)

$$B(\varphi_p) = \begin{bmatrix} \cos\varphi_p & 0 & \sin\varphi_p \\ 0 & 1 & 0 \\ -\sin\varphi_p & 0 & \cos\varphi_p \end{bmatrix}$$

$$C(\varphi_g) = \begin{bmatrix} \cos\varphi_g & -\sin\varphi_g & 0 \\ \sin\varphi_g & \cos\varphi_g & 0 \\ 0 & 0 & 1 \end{bmatrix}$$

Table 1 Dimensions of skew bevel gears

		Pinion	Gear
Number of teeth	z_p, z_g	18	116
Pitch circle diameter		264.1346 mm	1702.1302 mm
Pitch cone angle	λ_{p0}, λ_{g0}	8.8167 deg	81.1833 deg
Normal module	M_n	10.6764	
Mean cone distance	R_m	759.65 mm	
Pressure angle	α	14.5 deg	
Skew angle	β	15 deg	
Face width	*b*	203.2 mm	
Shaft angle		90 deg	
Backlash		0.4064 - 0.5588 mm	

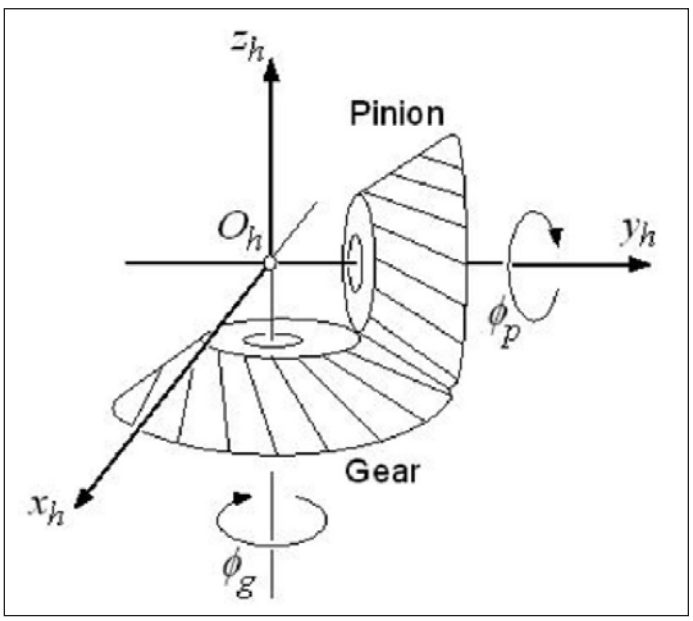

Figure 5 Meshing of pinion and gear.

Since $|n_p| = |n_g| = 1$, Equation14 represents a system of five scalar, non-linear equations with five unknowns — u_p, ψ_p, u_g, ψ_g and φ_g — considering angle φ_p as the input parameter. The continuous solution of the system of the non-linear equations permits the determination of the path of contact considering that φ_p changes every moment. A method of successive approximation is utilized in order to obtain a numerical solution of Equation 14. In this case it is convenient to use a cylindrical coordinate system.

The paths of contact on the pinion and gear tooth surfaces are represented by x_p (u_p, ψ_p) and x_g (u_g, ψ_g), respectively.

When the pinion is rotated by the angle φ_p the gear should be rotated by the angle $z_p/z_g\varphi_p$, assuming that pinion and gear are conjugate. Realistically, however, this is not the case, and transmission errors occur. The function of transmission errors is defined as:

$$\Delta\varphi_g(\varphi_p) = \varphi_g(\varphi_p) - \frac{z_p}{z_g}\varphi_p \quad (16)$$

where:

$\Delta\varphi_g$ = function of transmission error

Results of TCA. The tooth contact pattern and transmission errors of the pinion member model (Eq. 1) and existing gear

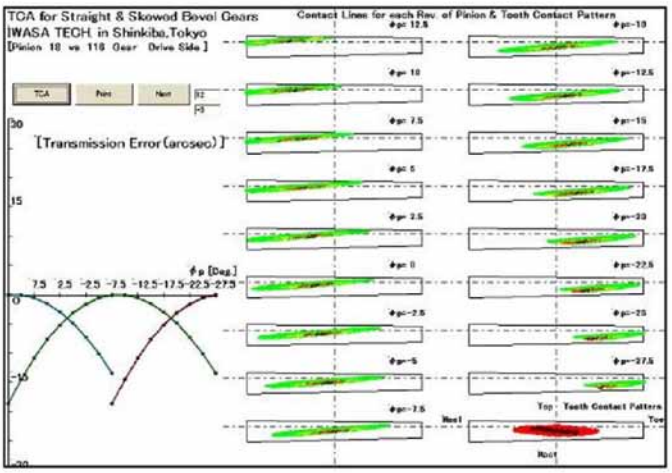

(a) Drive side

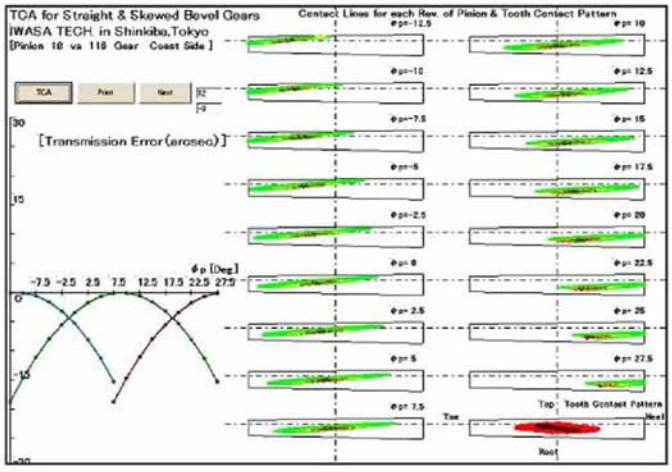

(b) Coast side

Figure 6 Analyzed results of tooth contact pattern and transmission errors without accounting for tooth surface form deviations.

member whose tooth surface is calculated under unloaded condition were analyzed based on the method used earlier.

Figure 6 shows the analyzed results of tooth contact pattern and transmission errors, without taking into account the tooth surface form deviations described earlier. Figure 6a is the result of drive-side, and Figure 6b is that of the coast-side. The amounts of tooth profile modification and crowning of pinion member are $\Delta c = 0.05$ mm and $\Delta s = 0.05$ mm — on both drive- and coast- sides — respectively. These values have influence on the tooth contact pattern and transmission errors, as mentioned. The right side from the center (Fig. 6) shows the analyzed contour line on the gear tooth surface at every instant when the rotation angle φ_p of the pinion changes from 12.5° to -27.5° on the drive-side, and from -12.5° to 27.5° on the coast-side. The lowest figure of the right side shows the total tooth contact pattern considering contact ratio. The region whose clearance between the pinion and gear tooth surfaces is less than 30 mm is displayed. The tooth contact patterns are obtained around the centers on the tooth surfaces of both drive- and coast-sides.

The left side (Fig. 6) shows the analyzed transmission errors. The shape of transmission errors is parabolic; the parabolic transmission errors occur due to the influence of both profile modification and crowning. In this case the rotation is transmitted smoothly. Therefore it is important to have the intersection before and after meshing. The maximum value of the transmission errors is about five arcsec of both drive- and coast-sides. These transmission errors can be adjusted by changing Δc and Δs.

Figures 6 and 7 show the analyzed results of tooth contact pattern and transmission errors with respect to the tooth surface form deviations. The amount of tooth profile modification and crowning of pinion member are $\Delta c = 0.1$ mm and $\Delta s = -0.4$ mm on the drive-side, and $\Delta c = 0.2$ mm and $\Delta s = 0.79$ mm on the coast-side. In addition, -0.4° in α and 0.05° in β on the drive-side and -0.25° in α, 0.03 degrees in β are changed. The tooth contact pattern deviates slightly from the center on the tooth surface of both drive- and coast-sides. These contact patterns seem to be acceptable in practical use. In addition, the transmission errors become large on the coast side. These transmission errors also seem to be acceptable in practical use.

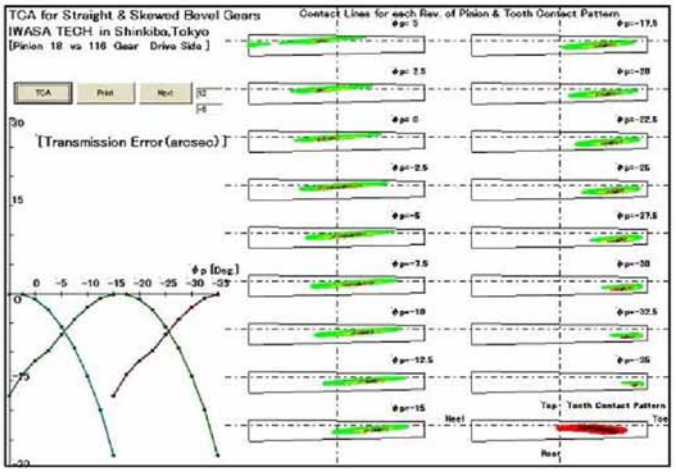

(a) Drive side

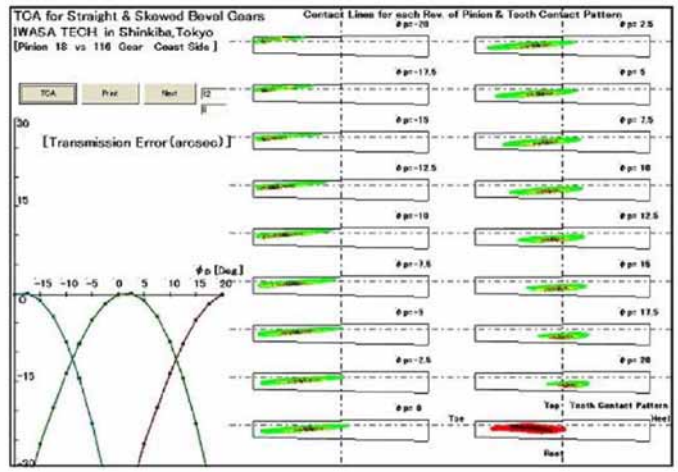

(b) Coast side

Figure 7 Analyzed results of tooth contact pattern and transmission errors with respect to tooth surface form deviations.

Manufacture of Pinion Member

The pinion member was manufactured using a 5-axis control machine (DMG Co., Ltd. DMU210P) based on the results of TCA. In this case the reference and hole surfaces, in addition to the tooth surfaces, can be machined and a tool approach provided from optimal direction using multi-axis control since the structure of the 2-axis of the inclination and rotation in addition to translational 3-axis are added; therefore, a thicker tool can be used. This should reduce the machining time and produce a smoother tooth surface. The radius end mills made of cemented carbide for a hard cutting tool were used in the machining of tooth surface. The number of edges is six and the diameter of end mill is 10 mm. Ball end mills were used in the machining of the tooth bottom. The number of the edges is six and the diameters of end mills are 10 mm and 5 mm, respectively, in the machining of the tooth bottom. The pinion material used was 18CrNiMo06. The tool pass was 1 mm for the large-sized pinion member. First, the pinion work was rough-cut and heat treated.

Afterward, the pinion member was semi-finished with the machining allowance of 0.3 mm after heat treatment. Finally, the pinion was finished with the machining allowance of 0.05 mm by swarf cutting. Machining with high accuracy and efficiency utilizing the advantages of a multi-axis control and multitasking machine tool in swarf cutting can be expected. Table 2 shows the conditions for semi-finishing and finishing of the pinion tooth surfaces. Figure 8 shows the situation of swarf cutting of the pinion member. The machining time of one side in rough-cutting is about 50 minutes; semi-finishing and finishing take about 170 minutes; the machining was finished without problems, such as defects of the end-mill.

Tooth Surface Form Error and Tooth Contact Pattern

The manufactured pinion tooth surfaces were measured using a CMM and compared with nominal data determined from the theoretical pinion tooth surface mating with the theoretical gear tooth surface—and without taking into account tooth surface form deviations. Figure 9 shows the measured result of the pinion member. Since tooth surface form deviations were not respected in the theoretical gear tooth surface, the tooth surface form errors are relatively large. In particular, the tooth surface form errors are large on the coast-side. The large-sized

Table 2 Conditions of pinion machining					
Processes	Diameter of end mill, mm	Revolution of main spindle, rpm	Feed, mm/min	Depth of cut, mm	Time/one side, min
Semi-finishing	10.0	1400	1100	0.2	120
Finishing	10.0	1600	1100	0.05	420

Figure 8 Swarf cutting of the pinion member.

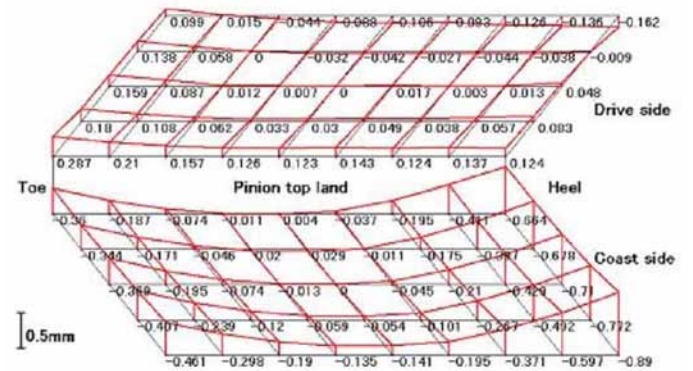

Figure 9 Measured result of the pinion member.

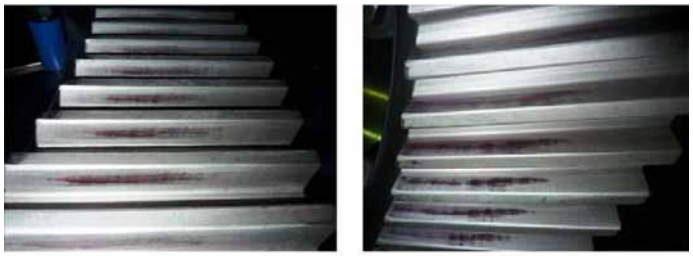

Figure 10 Experimental tooth contact patterns.

skew bevel gears were set on a gear meshing tester and the experimental tooth contact patterns were investigated. Figure 10 shows the result of the experimental tooth contact patterns on the gear tooth surface of the drive- and coast-sides, respectively. Although the experimental tooth contact pattern deviates from the center of the tooth surface slightly on both drive- and coast-sides, it is almost the same as that in Figure 7, with respect to the tooth surface deviations. From these results the validity of the manufacturing method of the pinion member using a multi-tasking machine was confirmed.

Conclusions

In this paper a manufacturing method of the pinion member of large-sized skew bevel gears using multi-axis control and multitasking machine tool respecting the existing gear member was proposed. The main conclusions obtained in this study are summarized as follows:

- The tooth surface forms of skew bevel gears were modeled mathematically.
- The deviations between the real and theoretical tooth surface forms were formalized using the measured coordinates of the real tooth surfaces of the gear member.
- The tooth surface form of the pinion member that has good performance mating with the existing gear member was determined using the results of tooth contact analysis.
- The pinion member was manufactured by swarf cutting using a multi-axis control and multitasking machine tool.
- The real tooth surfaces of the manufactured pinion member were measured using a CMM and the tooth surface form errors were detected.
- The experimental tooth contact patterns of the existing gear member and manufactured pinion member were compared with those of tooth contact analysis. As a result, there was good agreement.

References

1. Tsai Y.C. and Chin P.C. "Surface Geometry of Straight and Spiral Bevel Gears," *ASME Journal of Mechanisms, Transmissions and Automation in Design*, 1987, 109, pp. 443-449.
2. Townsend, D.P. *Dudley's Gear Handbook*, 2nd Edition, "Design, Manufacture and Application of Gears," McGraw-Hill, 1991 New York pp. 2.9–2.17.
3. Radzevich, S.P. *Handbook of Practical Gear Design and Manufacture*, 2nd Edition, CRC Press, 1984, p. 53.
4. Dimarogonas, A.D. *Machine Design: A CAD Approach*, Wiley-InterScience, 2001, pp. 869–874.
5. Davis, J.R. *Gear Materials, Properties and Manufacture*, 2005, ASM International Technical Books Committee, pp. 92–99.
6. Fuentes A., J.L. Iserte, I. Gonzales-Perez and F.T. Sanchez-Marin. *"Computerized Design of Advanced Straight- and Skew-Bevel Gears Produced by Precision Forging,"* 2011, "Computing Methods of Applied Mechanical Engineering," 2011, 200, pp. 2363–2377.
7. Nakaminami, M., T. Tokuma, T. Moriwaki and K. Nakamoto. "Optimal Structure Design Methodology for Compound Multi-Axis Machine Tools, Part I (Analysis of Requirements and Specifications)," *International Journal of Automation Technology*, Vol. I, No. 2, 2007, pp. 78–86.
8. Moriwaki T. "Multi-Functional Machine Tool," *Annals of CIRP*, Vol. 57, No. 2, 2008, pp. 736–749.
9. Kawasaki, K., I. Tsuji, Y. Abe and H. Gunbara. "Manufacturing Method of Large-Sized Spiral Bevel Gears in Cyclo-Palloid System Using Multi-Axis Control and Multi-Tasking Machine Tool, *Proceedings International Conference on Gears, Vol. I*, Garching, Germany, 2010, pp. 337–348, ***Gear Technology*** 2011 and ***Gear Technology India*** 2012.
10. Kawasaki K., I. Tsuji and H. Gunbara. "Tooth Contact Analysis and Manufacture on Multi-Tasking Machine of Large-Sized Straight Bevel Gears," *Proceedings ASME 2011 International Design Engineering Technical Conferences & Computers and Information in Engineering Conference*, 2011, Washington D.C., CD-ROM.
11. Sakai T. "A Study on the Tooth Profile of Hypoid Gears," *Trans. JSME*, Vol. 21, No. 102, 1955, pp. 164–170 (in Japanese).
12. Litvin, F.L. and A. Fuentes. *Gear Geometry and Applied Theory,* 2nd Ed., Cambridge University Press, 2004, UK, pp. 98–101.
13. Kawasaki, K. and I. Tsuji. "Analytical and Experimental Tooth Contact Pattern of Large-Sized Spiral Bevel Gears in Cyclo-Palloid System," *Trans. ASME Journal of Mechanical Design,* Vol.132, 041004–1–8, 2010.
14. Fan, Q., R.S. Da Foe and J.W. Swanger. "Higher-Order Tooth Flank Form Error Correction for Face-Milled, Spiral Bevel and Hypoid Gears," *Trans. ASME Journal of Mechanical Design,* Vol.130, 072601–1–7, 2008.
15. Stadtfeld, H.J. *Handbook of Bevel and Hypoid Gears: Calculation, Manufacturing and Optimization*, Rochester Institute of Technology, 1993, pp. 9–12.